

### Abstract

The PIP-II beam transfer line (BTL) transports the beam from the PIP-II Linac to the Booster synchrotron ring. A crucial aspect of the BTL design is the collimation system which play a vital role in removing large amplitude particles that may otherwise miss the horizontal and vertical edges of the foil at the point of injection into the Booster. To ensure the effectiveness of the collimators, simulations were conducted to determine optimal placement within the BTL. These simulations revealed that precise control of the accumulated phase advances between the collimators and the foil is critical. To achieve fine-tuning of the phase advance, a phase trombone was incorporated within the BTL. This paper presents the design and implementation details of this phase trombone.

### Introduction

- The Proton Improvement Plan II, or PIP-II, is an essential enhancement to the Fermilab accelerator complex, powering the world's most intense high-energy neutrino beam on its journey from Illinois to the Deep Underground Neutrino Experiment in South Dakota – 1,300 kilometres (800 miles) [1]. At the heart of PIP-II is a new 800 MeV linear accelerator, the Linac, based on superconducting radio-frequency technology.
- The linac accelerates H<sup>+</sup> ions for injection into the existing Booster ring, where they are converted into protons and accumulated by multi-turn charge exchange using a stripping foil. The protons are then accelerated to 8 GeV before being transferred into another ring downstream. Figure 1 shows the layout of the PIP-II Linac complex.

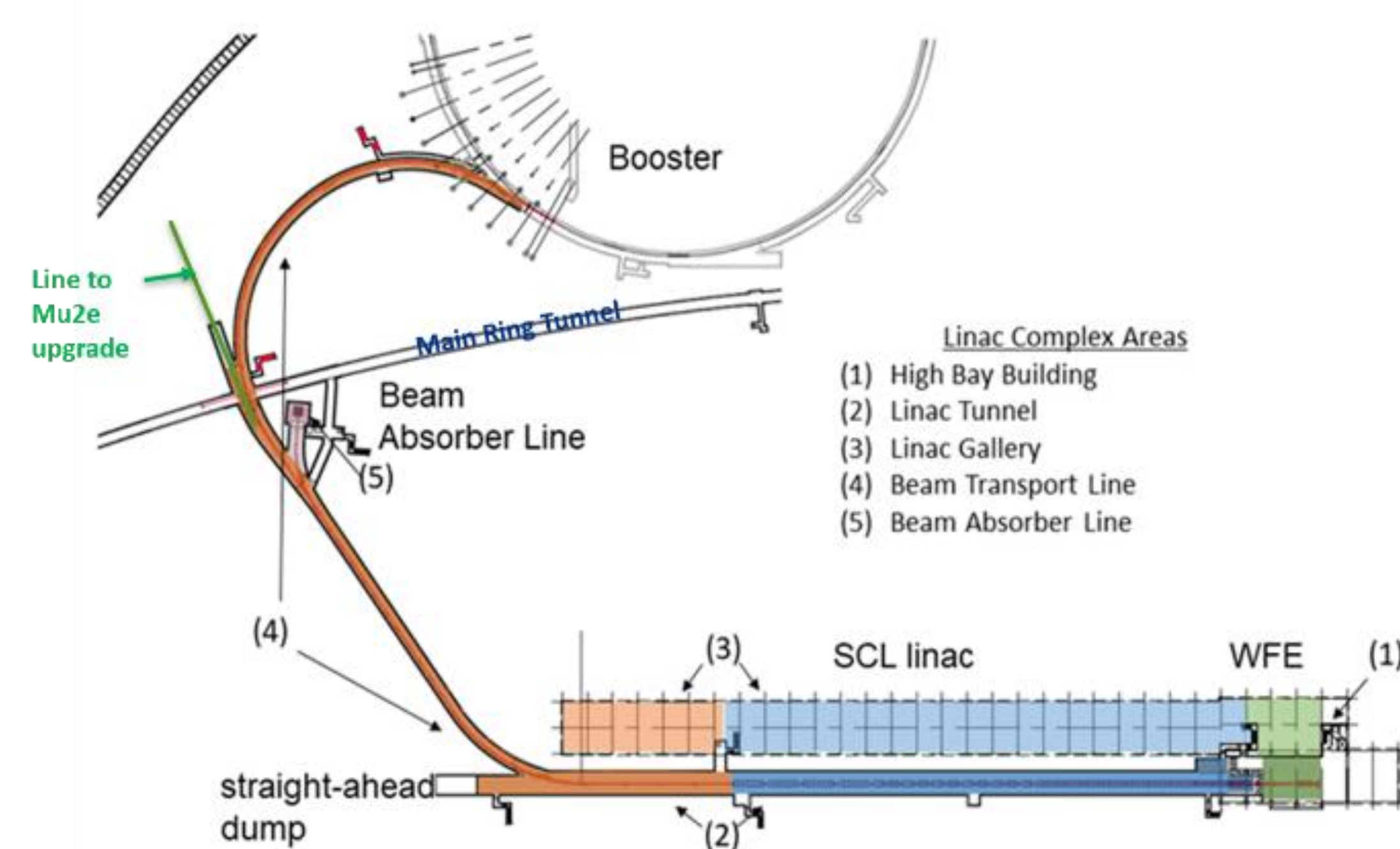


Figure 1: Layout of the PIP-II Linac Complex

The PIP-II Beam Transfer Line (BTL) transports the beam from the PIP-II Linac to the Booster ring. The optics of the BTL has recently been finalized [2]; a 3D CAD model is shown in Fig. 2. The lattice is based on 90-deg FODO cells. Four achromatic arcs, each comprising four cells are joined by an 8-cell straight section. The design meets requirements for civil construction and avoids mechanical interference with existing components. In an earlier design iteration, rolled dipoles in the second arc were used to bend the beam vertically; this feature has been eliminated and the reference trajectory now lies in a single plane. A switched magnet and corresponding septum are in Cell 3 and Cell 4 of the straight section and deflects the beam that would have gone to Booster into the Beam Absorber Line (BAL). A similar setting of a switched magnet and Septum will be located in Cell 7 and Cell 8 for a future upgrade which converts the 2-way split into a 3-way split providing the option of delivering beam to a Mu2e experiment.

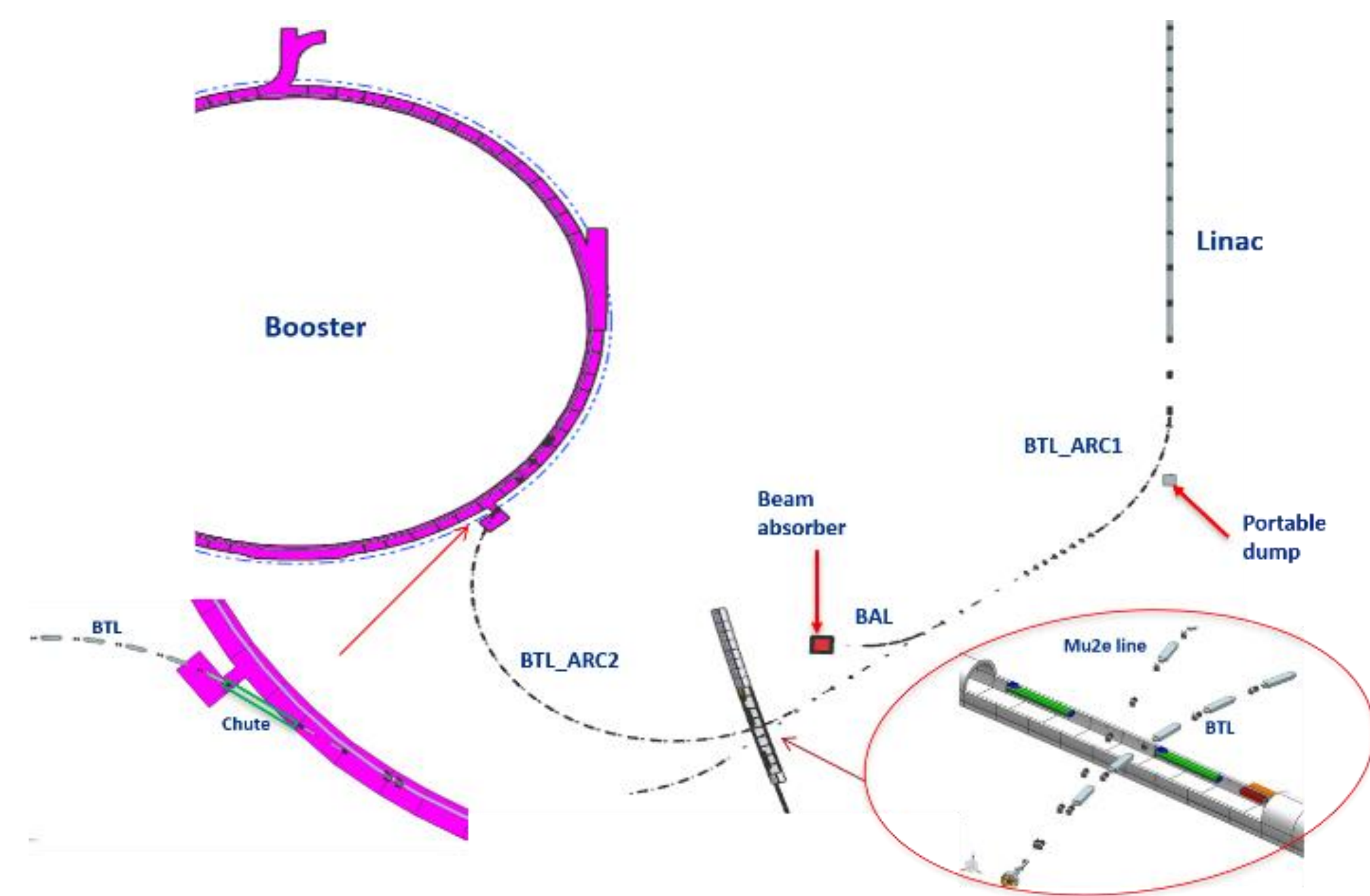


Figure 2: 3D CAD Model of the PIP-II complex layout.

### COLLIMATION IN THE BTL

- A crucial aspect of the BTL design is the collimation system [3]. To minimize the number of parasitic hits, the beam must be positioned as close as possible to the lower corner of the injection stripping foil. The minimal achievable distance is a compromise between the number of parasitic hits on the injection foil and the losses in the Booster injection absorber due to particles populating the distribution tails missing the foil.
- The role of the collimators is to remove large amplitude particles that might otherwise miss the horizontal and vertical edge of the foil at the point of the Booster injection. By collimating the far tails of the beam transverse spatial distribution in a controlled manner one can move the beam closer to the foil edge without causing an increase in losses. This is illustrated in Fig. 3.

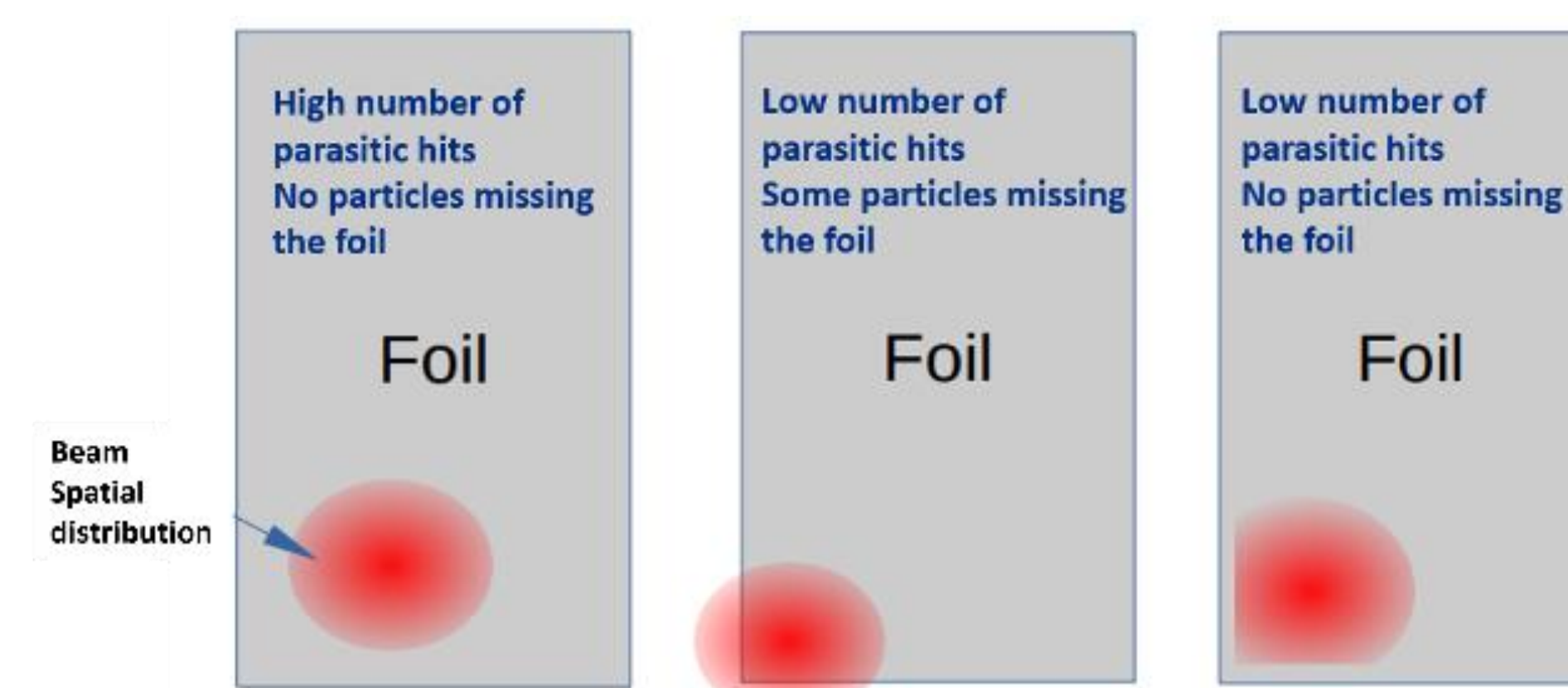


Figure 3: 3 cases of beam distribution at foil.

- To ensure the effectiveness of the collimators, simulations were conducted to optimize their optical placement within the BTL. One important constraint is that the accumulated phase advance between collimator and foil should be as close as possible to an integer multiple of  $\pi$ . Since collimation can be performed on either side (L/R or T/B), collimator locations that are (almost)  $\pi/2$  apart are (almost) equivalent. In the BTL, the total accumulated phase advance between collimator H/V locations and foil are not exact multiples of  $\pi$ . This phase advance depends on several factors: (1) Accounting for the space needed for a vacuum connection and the enclosure assembly, the primary collimator jaw must be positioned at least 650 mm (25 in) downstream of a quadrupole. (2) The phase advance per cell both within the BTL and in the arcs is very nearly but not exactly  $\pi/2$  (due to bending magnet edge focusing and space charge). These deviations from  $\pi/2$  accumulate over many cells. (3) The H/V phase advances from the last cell of the 2nd arc to the foil are constrained by matching requirements for the Booster painting scheme.
- The best candidate locations are the 8 dispersion-free FODO cells (16 half-cells) in the straight section between the two arcs. The quad-to-quad separation in each half-cell is approximately 5.5 m. Many of the straight section half-cells are claimed for instrumentation or for possible bunching cavities. After careful consideration of other needs and requirements, cell 1 was selected for vertical collimation, cell 2 for horizontal collimation. Collimator jaws are located approximately 635 mm (~ 25 in) downstream of the nearest upstream quadrupole. Simulated beam distributions with collimators are shown in Fig. 4. The particle distribution used is a “realistic” (and probably pessimistic) distribution with somewhat larger emittances and  $dp/p$  than the nominal specification obtained by start-to-end tracking in a linac with errors.

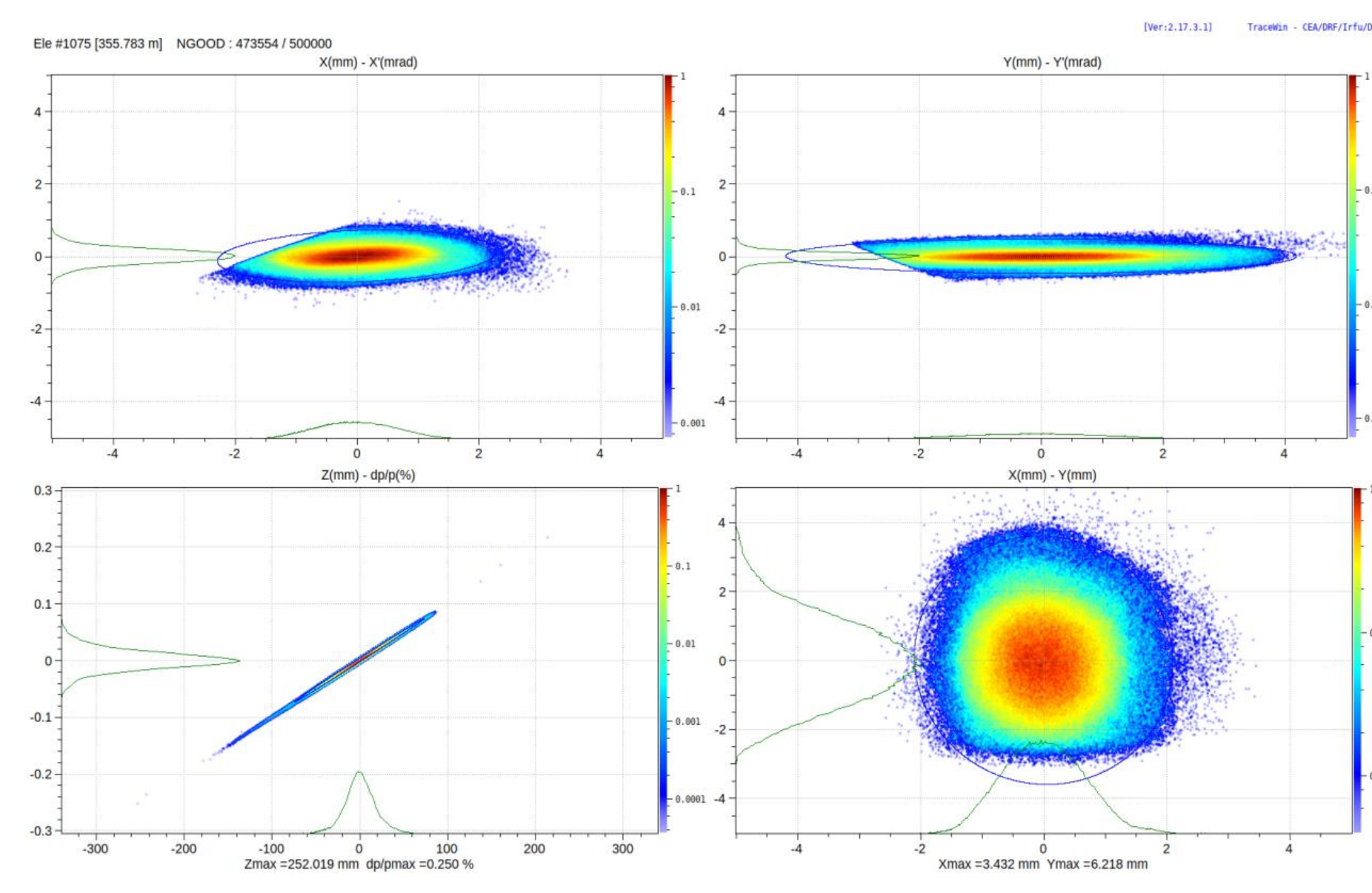


Figure 4: beam distribution with vertical collimator at cell 1 (2<sup>nd</sup> half cell) and Horizontal collimator at cell 2 (1<sup>st</sup> half cell). No phase advance correction.

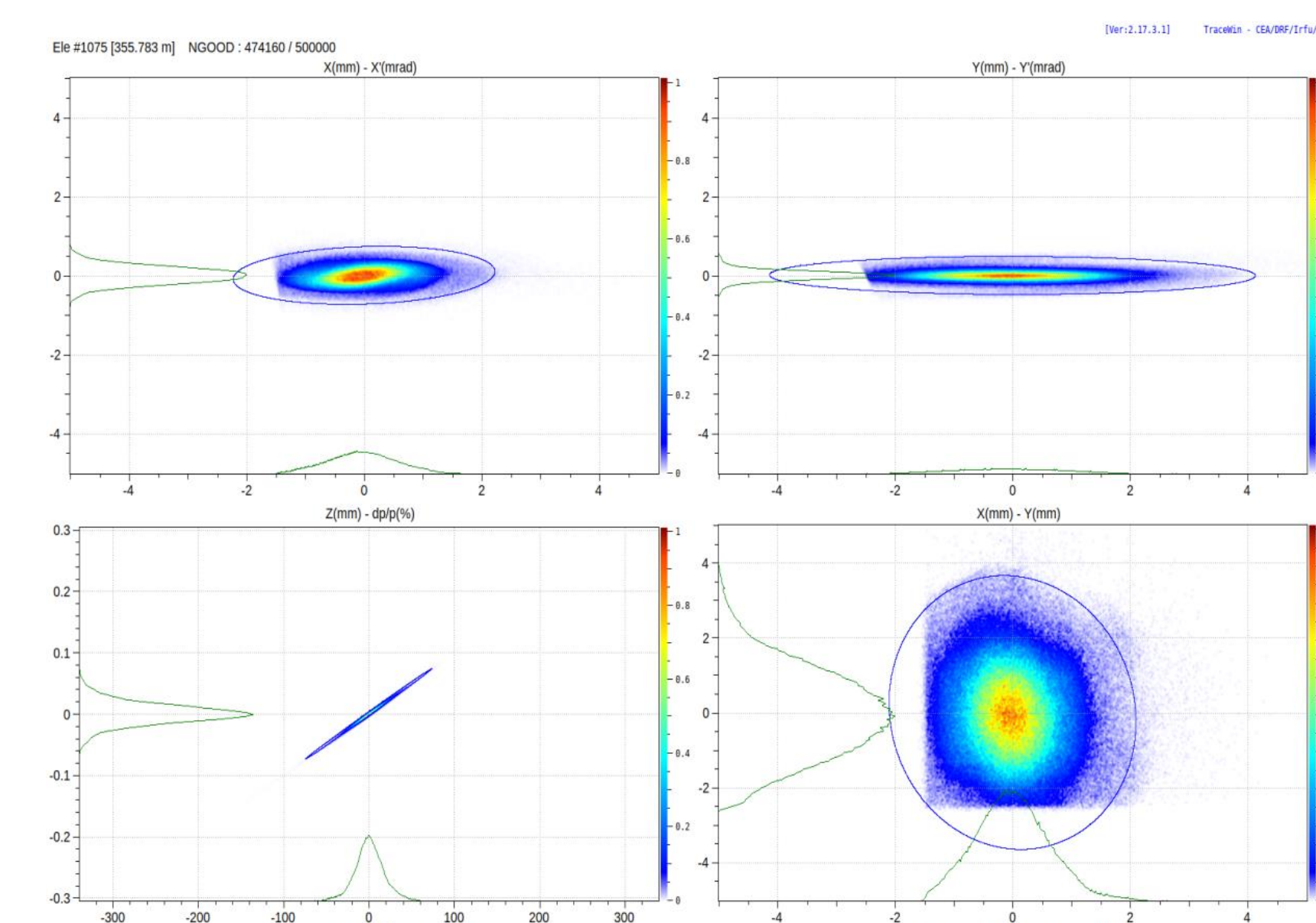


Figure 5: Distribution at foil after phase advance correction applied: -30° in Horizontal and +30° in vertical plane.

### PHASE ADVANCE CORRECTION

Figure 4 shows that even with optimal positioning of the collimators the spatial distribution edge at the foil with both horizontal and vertical collimators does not exhibit particularly sharply defined edges. The reason is that the accumulated phase advance determines the orientation of the collimator cut in the phase space plane at the foil location, but in the BTL base lattice, the accumulated phase advances between the collimators and the foil are not exactly an integer multiple of  $\pi$ . However, by adjusting the accumulated phase advances, a near ideal edge orientation in phase space can be achieved, as shown in Fig. 5.

### PHASE TROMBONE DESIGN

- There are 8 FODO cells in the BTL straight section lattice. The beta-functions within the straight are shown in Fig. 6 (solid line  $-\beta_x$ , dotted line  $-\beta_y$ ). Three FODO cells (cells 6,7,8, highlighted) will function as a phase trombone. Six individually powered quadrupoles allow the lattice functions to remain matched to their nominal design values at both upstream (cell 5 2nd half, marked A in RED) and downstream boundaries (2nd arc entrance, marked B in RED). Within the trombone region the  $\beta$ -functions may vary, allowing an adjustment of the phase advance accumulated between collimator locations and the foil.
- Two schemes, respectively dubbed symmetric and asymmetric, were investigated. It was found that the symmetric scheme results in more even beta-functions while the required quad strengths did not exceed the power supply range. Figure 7a presents the beta-functions within the trombone when the phase advance adjustment is set to  $d\mu_x = -30^\circ$  and  $d\mu_y = -60^\circ$ . Figure 7b shows the entire BTL lattice optics under the same conditions. Notably, the lattice outside the trombone section remains unchanged. The phase advance adjustment range of the phase trombone section is ( $\pm 90^\circ$ ,  $\pm 90^\circ$ ), in both horizontal and vertical planes. Table 1 lists the required strengths of the 6 quadrupoles and the maximum beta-functions in the trombone section for various phase advance settings.

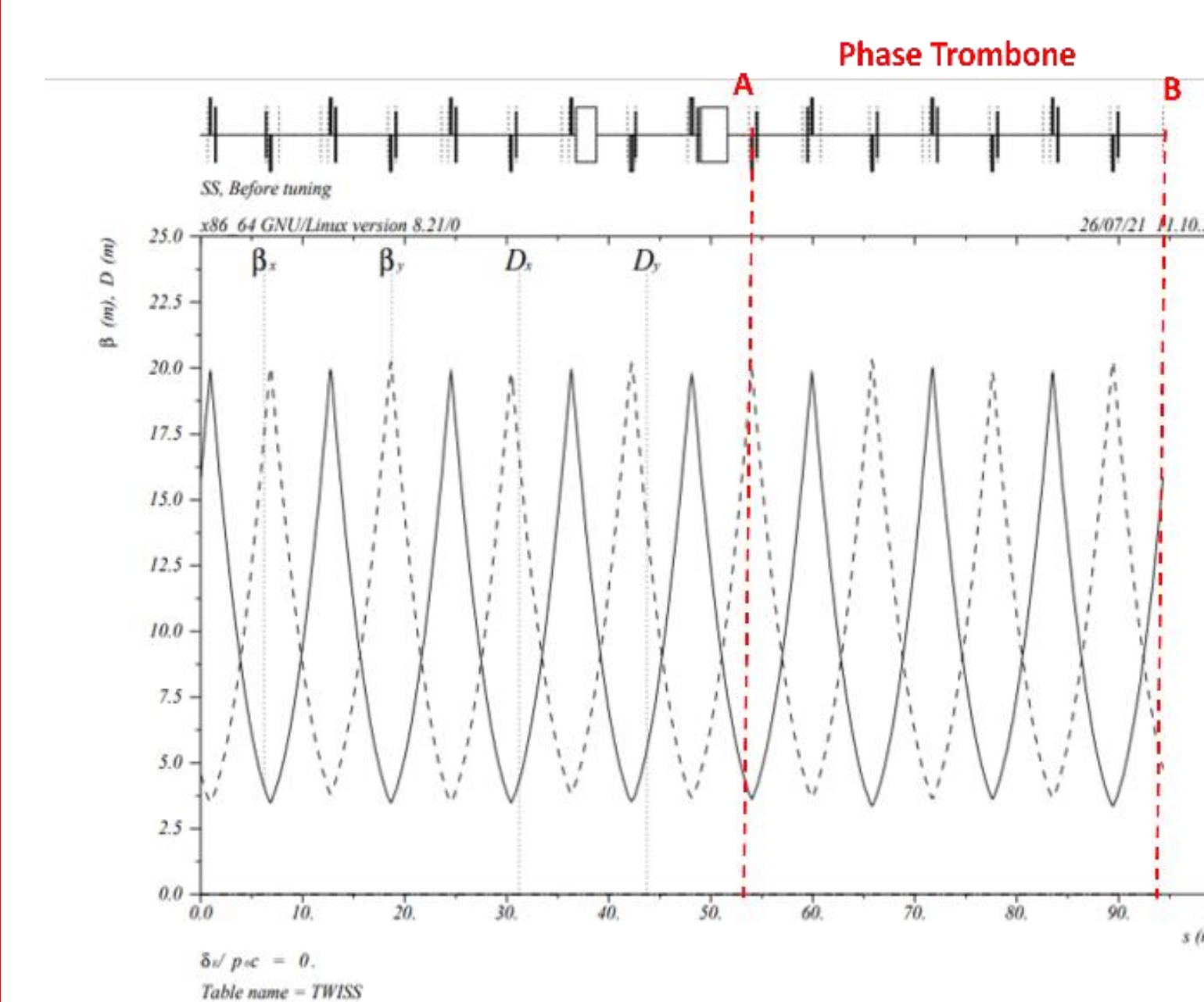


Figure 6: 8 FODO cells in the BTL lattice.

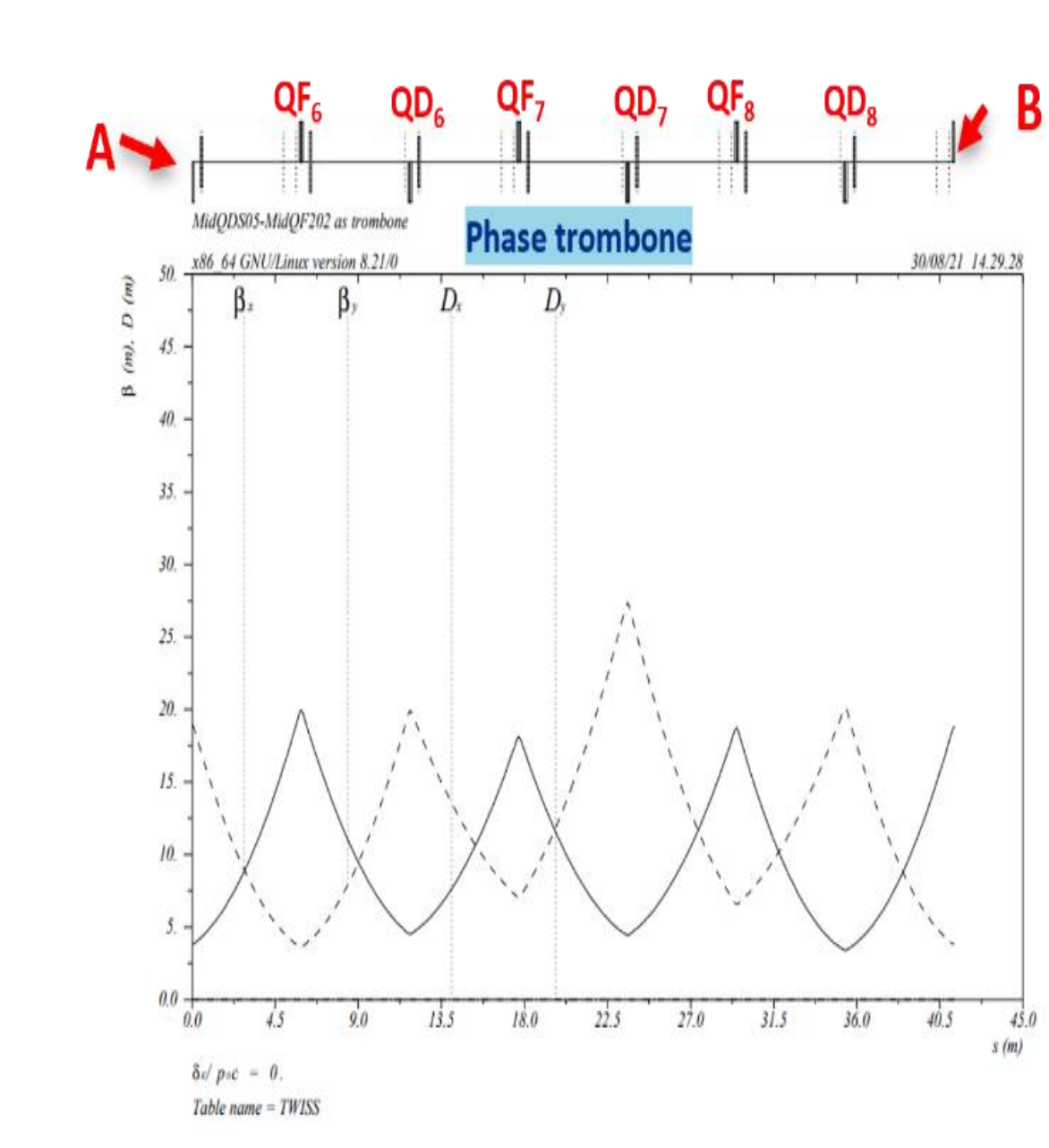


Figure 7a: Trombone in the BTL straight section; the phase advance adjustment of  $d\mu_x = -30^\circ$ ,  $d\mu_y = -60^\circ$ .

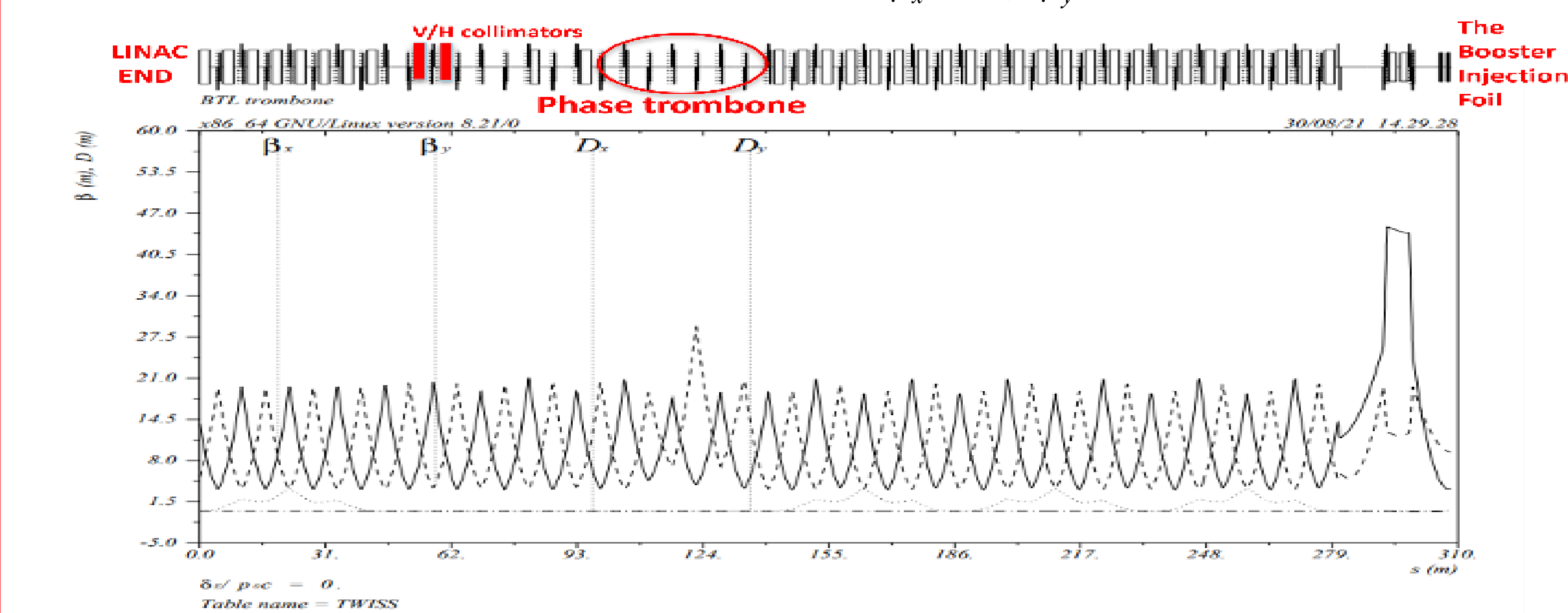


Figure 7b: Lattice of the BTL. the phase advance adjustment of  $d\mu_x = -30^\circ$ ,  $d\mu_y = -60^\circ$ .

Table 1: phase advance changes ( $d\mu_x, d\mu_y$ ) vs quads strengths, and the maximum  $\beta_x$  and  $\beta_y$

Adjusted phase/parameters	$(d\mu_x, d\mu_y)$ (Nominal)	$(d\mu_x, d\mu_y)$ (0, 0)	$(d\mu_x, d\mu_y)$ (20°, 20°)	$(d\mu_x, d\mu_y)$ (-20°, 20°)	$(d\mu_x, d\mu_y)$ (20°, -20°)	$(d\mu_x, d\mu_y)$ (0, 20°)	$(d\mu_x, d\mu_y)$ (20°, 0)	$(d\mu_x, d\mu_y)$ (32°, 32°)
$K_{Q6}$ (m <sup>-2</sup> )	1.209	1.209	1.248	1.153	1.234	1.056	1.354	1.273
$K_{Q6}$	-1.187	-1.221	-1.227	-1.202	-1.160	-1.138	-1.220	-1.259
$K_{Q7}$	1.209	1.192	1.305	1.130	1.278	1.195	1.315	1.347
$K_{Q7}$	-1.187	-1.186	-1.293	-1.266	-1.117	-1.112	-1.171	-1.338
$K_{Q8}$	1.209	1.214	1.281	1.195	1.268	1.364	1.176	1.307
$K_{Q8}$	-1.187	-1.150	-1.247	-1.241	-1.138	-1.137	-1.136	-1.264
$(\beta_x)_{max}$ (m)	19.969	20.441	21.137	20.866	19.982	25.000	21.166	22.431
$(\beta_y)_{max}$ (m)	20.268	21.144	21.123	21.125	21.146	22.972	21.147	21.588

### CONCLUSION

A phase trombone was incorporated in the BTL lattice. The phase advance adjustment range of this phase trombone section is ( $\pm 90^\circ$ ,  $\pm 90^\circ$ ), both in horizontal and vertical planes. By adjusting the accumulated phase advances between the collimators (both horizontal and vertical) and the foil at the Booster injection the trombone a near ideal sharp edge distribution can be achieved at the foil without perturbing matching to the Booster ring.

### REFERENCES

- PIP-II final design report.
- M. Xiao, “Lattice Design of the Beam Transfer Line (BTL) from PIP-II LINAC to the Booster at Fermilab”. <https://accelconf.web.cern.ch/ipac2021/doi/JACoW-IPAC2021-WEPAB211.html>
- D.E. Johnson, et. al., “BEAM COLLIMATION IN THE PIP-II LINAC TO BOOSTER TRANSFER LINE”. <https://accelconf.web.cern.ch/ipac2021/papers/THPAB158.pdf>